References

[1]Vorreiter, J. W., and Shepard, C. E., "Performance Characteristics of the Constricted-Arc Supersonic Jet," *Proceedings of the Heat Transfer and Fluid Mechanics Institute*, edited by A. F. Charwat, Stanford Univ., Stanford, CA, June 1965, pp. 42–49.

[2]Shepard, C. E., Watson, V. R., and Stine, H. A., "Evaluation of a Constricted-Arc Supersonic Jet," NASA TN D-2066, Jan. 1964.

[3]Shepard, C. E., Ketner, D. M., and Vorreiter, J. W., "A High-Enthalpy Plasma Generator for Entry Heating Simulation," NASA TN D-4583, May 1968.

[4]Winovich, W., and Carlson, W. C. A., "The 60-MW Shuttle Interaction Heating Facility," *Proceedings of the 25th International Instrumentation Symposium*, Instrument Society of America, Pittsburg, PA, May 1979, pp. 59–75.

[5]Winovich, W., and Carlson, W. C. A., "The Giant Planet Facility," presented at the 25th International Instrumentation Symposium, Anaheim, CA, May 1979.

[6]Winovich, W., Balboni, J., and Balakrishnan, A., "Application of Numerical Simulation to Enhance Arcjet Performance Simulation," *Thermophysical Aspects of Reentry Flows*, edited by J. N. Moss and C. D. Scott, Vol. 103, Progress in Aeronautics and Astronautics, AIAA, New York, 1986, pp. 393–415.

[7]Watson, V. R., and Pegot, E. B., "Numerical Calculations for the Characteristics of a Gas Flowing Axially Through a Constricted Arc," NASA TN D-4042, June 1967.

[8]Nicolet, W. E., Shepard, C. E., Clark, K. J., Balakrishnan, A., Kesselring, J. P., Suchsland, K. E., and Reese, J. J., "Methods for the Analysis of High-Pressure, High-Enthalpy Arc Heaters," AIAA Paper 75-704, Denver, CO, May 1975.

[9]Nicolet, W. E., Shepard, C. E., Clark, K. J., Balakrishnan, A., Kesselring, J. P., Suchsland, K. E., and Reese, J. J., "Analytical and Design Study for a High-Pressure, High-Enthalpy Constricted Arc Heater," Arnold Engineering Development Center, TR-75-47, July 1975.

[10]Park, C., "Calculation of Nonequilibrium Radiation in the Flight Regimes of Aeroassisted Orbital Transfer Vehicles," *Thermal Design of Aeroassisted Orbital Transfer Vehicles*, edited by H. F. Nelson, Vol. 96, Progress in Astronautics and Aeronautics, AIAA, New York, 1985, pp. 395–418.

[11]Park, C., "Nonequilibrium Air Radiation (NEQAIR) Program: User's Manual," NASA TM 86707, July 1985.

[12]Liu, Y., and Vinokur, M., "Equilibrium Gas Flow Computations. Part 1: Accurate and Efficient Calculation of Equilibrium Gas Properties," AIAA Paper 89-1736, Buffalo, NY, June 1989.

Source Function Approach for Radiative Heat Transfer Analysis

J. Huan* and M. H. N. Naraghi†

Manhattan College, Riverdale, New York 10471

Introduction

THIS note presents a source function approach for analysis of three-dimensional radiative heat transfer in absorbing, emitting, and anisotropically scattering media. Two integral equations relating the source function for the gas and leaving intensity for surfaces are developed incorporating direct exchange factors between differential elements. The resulting equations are then discretized using a numerical scheme. Numerical results based on the present approach are presented for a three-dimensional idealized furnace model, which are in excellent agreement with the existing solutions.

Received April 5, 1991; revision received Oct. 28, 1991; accepted for publication Nov. 1, 1991.

*Graduate Assistant, Department of Mechanical Engineering.

†Associate Professor, Department of Mechanical Engineering. Member AIAA.

Formulation

Consider a multidimensional diffuse boundary enclosure containing absorbing, emitting, and anisotropically scattering media, as shown in Fig. 1. Neglecting the conductive and convective heat transfer effects, the following integral equations can be derived for radiative heat transfer in the enclosure (see Ref. 1 for derivations)

$$I_s(\mathbf{r}) = \varepsilon i_{bs}(\mathbf{r}) + \frac{\rho}{\pi}\int_{2\pi} I_s(\mathbf{r}')\tau(|\mathbf{r}-\mathbf{r}'|)\cos\theta_r\, d\Omega' + \frac{\rho}{\pi}\int_{2\pi}\int_0^{|r-r'|} I_g(\mathbf{r}_l,\Omega')\tau(|\mathbf{r}-\mathbf{r}_l|)\cos\theta_r K_t\, dl\, d\Omega' \quad (1)$$

$$I_g(\mathbf{r},\Omega) = \frac{q_g'''(\mathbf{r})}{4\pi K_t} + \frac{1}{4\pi}\int_{4\pi} I_s(\mathbf{r}')\tau(|\mathbf{r}-\mathbf{r}'|)\times[\omega_0\Phi(\Omega',\Omega)-\omega_0+1]\, d\Omega' + \frac{1}{4\pi}\int_{4\pi}\int_0^{|r-r'|} I_g(\mathbf{r}_l,\Omega')\tau(|\mathbf{r}-\mathbf{r}_l|)\cdot[\omega_0\Phi(\Omega',\Omega)-\omega_0+1]K_t\, dl\, d\Omega' \quad (2)$$

$$q_s''(\mathbf{r}) = \varepsilon E_{bs}(\mathbf{r}) - \varepsilon\int_{2\pi} I_s(\mathbf{r}')\tau(|\mathbf{r}-\mathbf{r}'|)\cos\theta_r\, d\Omega' - \varepsilon\int_{2\pi}\int_0^{|r-r'|} I_g(\mathbf{r}_l,\Omega')\tau(|\mathbf{r}-\mathbf{r}_l|)\cos\theta_r K_t\, dl\, d\Omega' \quad (3)$$

$$4(1-\omega_0)E_{bg}(\mathbf{r}) = \frac{q_g'''(\mathbf{r})}{K_t} + (1-\omega_0)\int_{4\pi} I_s(\mathbf{r}')\tau(|\mathbf{r}-\mathbf{r}'|)\, d\Omega' + (1+\omega_0)\int_{4\pi}\int_0^{|r-r'|} I_g(\mathbf{r}_l,\Omega')\tau(|\mathbf{r}-\mathbf{r}_l|)K_t\, dl\, d\Omega' \quad (4)$$

where $\mathbf{r}_l = \mathbf{r}' + l(\mathbf{r}-\mathbf{r}')/|\mathbf{r}-\mathbf{r}'|$, $\tau(|\mathbf{r}-\mathbf{r}'|) = \exp(-K_t|\mathbf{r}-\mathbf{r}'|)$ is the transmittance between location $\mathbf{r}$ and $\mathbf{r}'$, I_g is

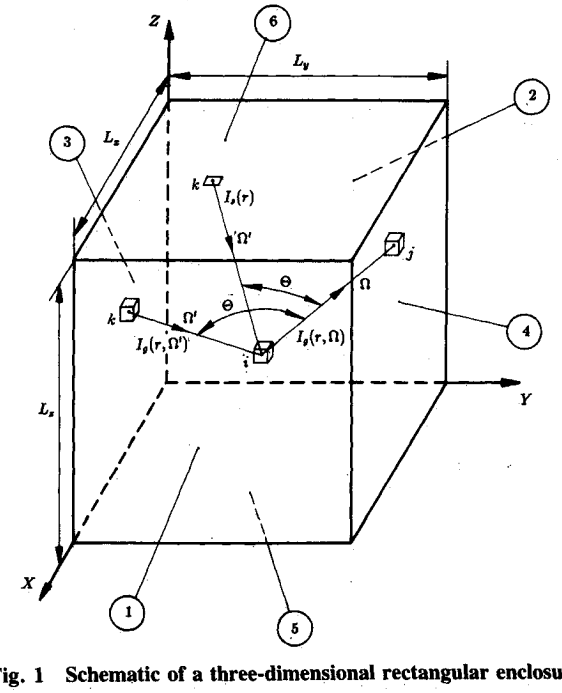

Fig. 1 Schematic of a three-dimensional rectangular enclosure.

gas source function and I_s is surface leaving intensity. The differential solid angle $d\Omega$ can be expressed by $d\Omega = \cos\theta\, dA/r^2$. Using this expression, the angular and line integrals in Eqs. (1–4) can be converted into surface and volume integrals, and making use of the direct exchange factors between surface and gas differential elements as shown in Ref. 2 [$\overline{dss}(\mathbf{r}_i, \mathbf{r}_j) = \cos\theta_i \cos\theta_j \tau(\mathbf{r}_{ij})\, dA_j/(\pi|\mathbf{r}_{ij}|^2)$, $\overline{dsg}(\mathbf{r}_i, \mathbf{r}_j) = K_t \cos\theta_i \tau(\mathbf{r}_{ij})\, dV_j/(\pi|\mathbf{r}_{ij}|^2)$, $\overline{dgs}(\mathbf{r}_i, \mathbf{r}_j) = \cos\theta_j \tau(\mathbf{r}_{ij})\, dA_j/(4\pi|\mathbf{r}_{ij}|^2)$ and $\overline{dgg}(\mathbf{r}_i, \mathbf{r}_j) = K_t \tau(\mathbf{r}_{ij})\, dV_j/(4\pi|\mathbf{r}_{ij}|^2)$], the resulting equations become

$$I_s(\mathbf{r}) = \varepsilon E_{bs}(\mathbf{r})/\pi + \rho \int_A I_s(\mathbf{r}')\, \overline{dss}(\mathbf{r}, \mathbf{r}') + \rho \int_V I_g(\mathbf{r}', \Omega')\, \overline{dsg}(\mathbf{r}, \mathbf{r}') \tag{5}$$

$$I_g(\mathbf{r}, \Omega) = \frac{q'''_g(\mathbf{r})}{4\pi K_t} + \int_A I_s(\mathbf{r}')[\omega_0 \Phi(\Omega', \Omega) - \omega_0 + 1]\, \overline{dgs}(\mathbf{r}, \mathbf{r}') + \int_V I_g(\mathbf{r}', \Omega') \times [\omega_0 \Phi(\Omega', \Omega) - \omega_0 + 1]\, \overline{dgg}(\mathbf{r}, \mathbf{r}') \tag{6}$$

$$q''_s(\mathbf{r}) = \varepsilon E_{bs}(\mathbf{r}) - \varepsilon\pi \int_A I_s(\mathbf{r}')\, \overline{dss}(\mathbf{r}, \mathbf{r}') - \varepsilon\pi \int_V I_g(\mathbf{r}', \Omega')\, \overline{dsg}(\mathbf{r}, \mathbf{r}') \tag{7}$$

$$E_{bg}(\mathbf{r}) = \frac{q'''_g(\mathbf{r})}{4K_t(1 - \omega_0)} + \pi \int_A I_s(\mathbf{r}')\, \overline{dgs}(\mathbf{r}, \mathbf{r}') + \pi \int_V I_g(\mathbf{r}', \Omega')\, \overline{dgg}(\mathbf{r}, \mathbf{r}') \tag{8}$$

If the surface emissive power $E_s(\mathbf{r})$ and gas heat source $q'''_g(\mathbf{r})$ are known, Eqs. (5) and (6) are used to find the surface leaving intensity $I_s(\mathbf{r})$ and source function $I_g(\mathbf{r}, \Omega)$. Then, Eqs. (7) and (8) are implemented to determine the surface flux, $q''_s(\mathbf{r})$, and gas black emissive power $E_{bg}(\mathbf{r}) = \sigma T^4(\mathbf{r})$.

Numerical integration schemes such as Gaussian quadrature, Simpson, trapezoidal, or rectangular (midpoint) integration method are utilized to discretize Eqs. (5–8). The Guassian quadrature discretization provides the most accurate results; however, since the nodal points in this method are not evenly located, it is undesirable for combined conduction-convection-radiation problems where a finite difference compatible grid is needed. For these types of problems, Simpson, trapezoidal and rectangular (midpoint) methods are more appropriate. Discretizing Eqs. (5–8) using any of the numerical integral schemes, we obtain

$$I_{s_i} = \varepsilon i_{bs_i} + \rho \sum_{j=1}^{N_s} w_{s_j} I_{s_j}\, \overline{ds_i s_j} + \rho \sum_{j=1}^{N_g} w_{g_j} I_{g_{j,i}}\, \overline{ds_i g_j} \tag{9}$$

$$I_{g_{i,j}} = \frac{q'''_{g_i}}{4\pi K_t} + \sum_{k=1}^{N_s} w_{s_k} I_{s_k}[\omega_0 \Phi_{k,i,j} - \omega_0 + 1]\, \overline{dg_i s_k} + \sum_{k=1}^{N_g} \omega_{g_k} I_{g_{k,i}}[\omega_0 \Phi_{k,i,j} - \omega_0 + 1]\, \overline{dg_i g_k} \tag{10}$$

$$q''_{s_i} = \varepsilon E_{bs_i} - \varepsilon\pi \sum_{j=1}^{N_s} \omega_{s_j} I_{s_i}\, \overline{ds_i s_j} - \varepsilon\pi \sum_{j=1}^{N_g} \omega_{g_j} I_{g_{j,i}}\, \overline{ds_i g_j} \tag{11}$$

$$E_{bg_i} = \frac{q'''_{g_i}}{4(1 - \omega_0)K_t} + \pi \sum_{j=1}^{N_s} \omega_{s_j} I_{s_j}\, \overline{dg_i s_j} + \pi \sum_{j=1}^{N_g} \omega_{g_j} I_{g_{j,i}}\, \overline{dg_i g_j} \tag{12}$$

In the above equations I_{s_j} represents leaving intensity from surface node j and $I_{g_{j,i}}$ represents source function of gas node j directed toward gas node i.

In many practical problems, the surface temperature (surface emissive power) and gas heat source are known. For these problems, Eqs. (9) and (10) are written for all surface and gas nodes and solved simultaneously to determine leaving intensity I_{s_i} and source function $I_{g_{i,j}}$. Then, these results are used in Eqs. (11) and (12) to determine surface heat flux and gas black emissive power (temperature). For isotropically scattering media, the phase function $\Phi(\Omega', \Omega) = 1$, and the above equations identically reduce to the so-called "radiosity-type" equations given in Ref. 3. There is, however, one major difference between the present approach and that of the zonal method. The exchange factors in the zonal formulation are between finite volumes and surfaces, while in the present approach, they are between nodes. Thus, substantial computaton efforts can be saved in the present approach. As will be shown, the use of exchange factor between nodes instead of finite volumes and surfaces will not sacrifice accuracy.

Results and Discussion

In order to illustrate the accuracy of the present method, the results based on the present method are benchmarked against the existing solutions based on the zonal method[4] and discrete exchange factor method (DEF)[5] for isotropic scattering medium cases, and the discrete-ordinates method,[6] N-bounce method[7] and P-3 method[8] for anisotropic scattering media.

Isotropic Scattering Media

Consider the unit cubical enclosure as shown in Fig. 1. The gas and surface conditions for this problem are: extinction coefficient $K_t = 1.0\ \mathrm{m}^{-1}$, heat source $q'''_g/E_{\mathrm{ref}} = 4$, scattering albedo $\omega_0 = 0.75$, surface emissivity $\varepsilon = 1.0$ (black surface), and surface emissive powers $E_1/E_{\mathrm{ref}} = E_3/E_{\mathrm{ref}} = E_6/E_{\mathrm{ref}} = 1.0$ and $E_2/E_{\mathrm{ref}} = E_4/E_{\mathrm{ref}} = E_5/E_{\mathrm{ref}} = 0.0$. This problem was also analyzed by Larsen[4] using the zonal method. For comparison purpose, the same grid size as that of the zonal method is used here (i.e., $5 \times 5 \times 5$), and the rectangular (midpoint) integration method is utilized. The results for surface heat fluxes and gas temperatures are given in Table 1. Table 2 shows the same results when $\omega_0 = 0.0$, $\varepsilon = 0.3$ and surfaces are cold. The results presented in Tables 1 and 2 show that the relative difference between the results based on the present method and the zonal method[4] is less than 1.0%, except for the heat flux at corner nodes. The CPU time performed on an IBM/RT model 130 workstation is 43 s.

Table 1 A comparison between the results of present method and the zonal method (three-dimensional enclosure, $\omega_0 = 0.75$, black walls and $q'''_g/E_{\mathrm{ref}} = 4.0$)

	Position	Present method	Zone method
Cold surface dimensionless heat flux	0.1	−0.946	−0.940
	0.3	−1.198	−1.211
	0.5	−1.337	−1.341
	0.7	−1.382	−1.387
	0.9	−1.344	−1.341
Hot surface dimensionless heat flux	0.1	0.038	0.051
	0.3	−0.223	−0.235
	0.5	−0.363	−0.368
	0.7	−0.407	−0.412
	0.9	−0.359	−0.350
Centerline dimensionless gas temperature	0.1	1.485	1.482
	0.3	1.503	1.501
	0.5	1.513	1.510
	0.7	1.516	1.514
	0.9	1.515	1.512

Table 2 A comparison between the results of present method and the zonal method (three-dimensional enclosure, $\omega_0 = 0$, $\varepsilon = 0.3$ and $q_g'''/E_{ref} = 4.0$)

	Position	Present method	Zone method
Surface dimensionless heat flux	0.1	−0.667	−0.664
	0.3	−0.716	−0.719
	0.5	−0.732	−0.733
Centerline dimensionless gas temperature	0.1	1.335	1.331
	0.3	1.346	1.343
	0.5	1.350	1.347

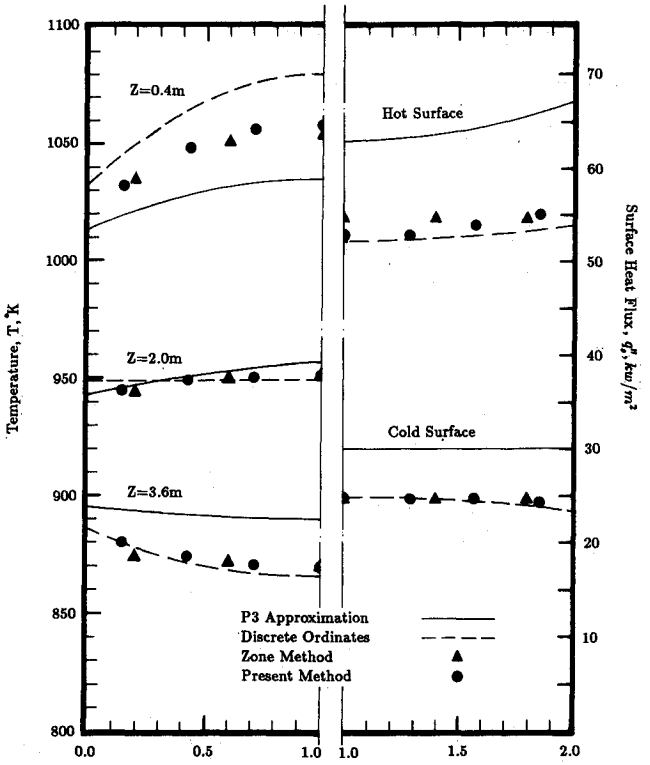

Fig. 2 Comparison of the surface heat flux and medium temperature based on the present method, the zonal method, P-3 approximation and discrete-ordinates method for a three-dimensional enclosure.

Next, consideration is given to an idealized furnace model that was presented by Mengüç and Viskanta.[8] The model has a rectangular parallel-piped configuration with the following specifications, $L_x = 2$ m, $L_y = 2$ m, $L_z = 4$ m, $K_t = 0.5$ m^{-1}, $\omega_0 = 0.0$ m^{-1}, $q_g''' = 5$ kw/m^3; and at the surfaces, $T_1 = T_2 = T_3 = T_4 = 900$ K, $\varepsilon_1 = \varepsilon_2 = \varepsilon_3 = \varepsilon_4 = 0.7$, $T_5 = 1200$ K, $\varepsilon_5 = 0.85$, $T_6 = 400$ K, $\varepsilon_6 = 0.7$. This enclosure was analyzed by Mengüç and Viskanta[8] using the P-3 approximation and zonal method; Fiveland,[6] using the discrete-ordinates method; and Naraghi and Huan,[7] using an N-bounce method. The resulting surface heat fluxes and gas temperatures based on the P-3, zonal, discrete-ordinate and the one- and two-bounce solutions are presented in Fig. 2. The results of the present method are based on a 7 × 7 × 10 grid. As shown in these figures, the results of the present method and zonal method are nearly coincident, especially for gas temperatures; however, there are some discrepancies between the results of discrete-ordinates, P-3 approximation and those of the zonal method.

Note that the results obtained based on the present method, for all isotropically scattering cases studied here, are identical to those based on DEF method.[5] Although the mathematical formulations of the DEF method and the present approach are totally different, their final results are exactly the same because both methods use identical exchange factors between nodes.

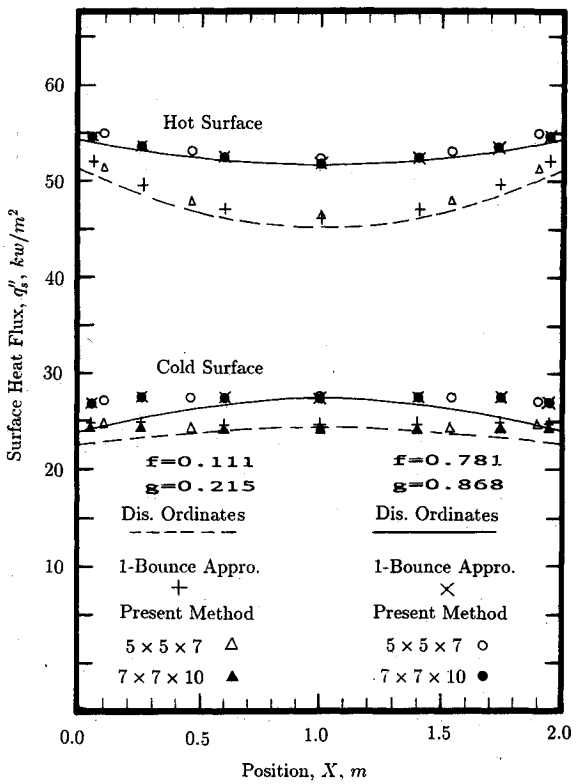

Fig. 3 Comparison of the surface flux results based on the present method and discrete-ordinates method for some δ-function phase functions.

Anisotropic Scattering Media

Recently, Fiveland[6] used the discrete-ordinates method for analysis of radiative heat transfer in three-dimensional enclosure with anisotropic scattering media. In Fiveland's work, a δ-Eddington approximation of the scattering phase function was utilized. To demonstrate the application of the present method to anisotropic scattering problems, the same problem is analyzed here. An equivalent form to the δ-Eddington approximation phase function can be written as

$$\Phi^*(\Theta) = 1 + 3X_1^* \cos\Theta \tag{13}$$

with modified

$$K_t^* = K_t(1 - f\omega_0) \tag{14}$$

$$\omega_0^* = \frac{\omega_0(1 - f)}{1 - f\omega_0} \tag{15}$$

Two cases are evaluated by the present method. The anisotropic parameters for these cases are listed as, for case 1, $f = 0.111$, $X_1^* = 0.215$; and for case 2, $f = 0.781$, $X_1^* = 0.868$. The radiative properties of the gas and surface are: $\omega_0 = 0.5$; $K_t = 1.0$ m^{-1} and $\varepsilon = 0.8$. Other enclosure specifications are the same as the idealized furnace model considered in the previous isotropic scattering case. Two grid sizes are used: 5 × 5 × 7, and 7 × 7 × 10. The resulting wall heat fluxes are presented in Fig. 3. As shown in this figure, the results of both grid sizes are so close that they cannot be distinguished from the figure. This might be due to the utilization of Gaussian quadrature integration, which provides accurate results even when a small number of nodes is used. Both results are in excellent agreement with those provided by the discrete-ordinates method,[6] and almost coincident with the results based on the one-bounce model.[7]

Conclusion

Integral equations relating the source function, emissive power, and heat source for gas, and leaving intensity, emissive power, and heat flux for surfaces are developed for anisotropically scattering media. When the gas scatters isotropically and surfaces are diffuse, these equations are reduced to the radiosity formulations given by Hottel and Sarofim.[3] The source function distribution in gas and leaving intensity distribution on surface can be obtained by solving the discrete form of these equations. The present method can be used for radiative heat transfer analysis of isotropic or anisotropic scattering media, and the results are in good agreement with those of the existing methods. The computational time is reasonably low for isotropically scattering problems. For anisotropically scattering cases, however, the computational time can become quite high.

In the zonal method, the radiosities are net radiative energy leaving finite gas volumes and finite surface areas. To calculate these radiosites, direct exchange areas between finite volume and surfaces must be evaluated. Substantial computational efforts are usually used to evaluate multiple integrations of the exchange areas. In the present approach, however, the exchange factors between nodal points are used. Consequently, substantial computational time can be saved by avoiding multiple integrations in the exchange factor computation without sacrificing the accuracy.

Most recently, Saltiel and Naraghi[9-10] have demonstrated that by using a rectangular (midpoint) numerical integration method, the DEF method can be applied to geometrically complex problems. Because the exchange factors and numerical discretization method used in the present approach is the same as DEF method, the present method can also be easily applied to geometrically complex problems.

References

[1]Huan, J., and Naraghi, M. H. N., "Analysis of Radiative Heat Transfer in Three Dimensional Absorbing, Emitting, and Scattering Media—A Source Function Approach," *Radiation Heat Transfer*, edited by S. T. Thynell and J. R. Mahan, American Society of Mechanical Engineers Publication HTD-Vol. 154, Presented at the American Society of Mechanical Engineers Winter Annual Meeting, Dallas, TX, Nov. 25–30, 1990, pp. 59–66.

[2]Naraghi, M. H. N., Chung, B. T. F., and Litkouhi, B., "A Continuous Exchange Factor Method for Radiative Exchange in Enclosures with Participating Media," *Journal of Heat Transfer*, Vol. 110, No. 2, 1988, pp. 456–462.

[3]Hottel, H. C., and Sarofim, A. F., *Radiative Transfer*, McGraw-Hill, New York, 1967.

[4]Larsen, M. E., "Exchange Factor Method and Alternative Zonal Formulation for Analysis of Radiating Enclosures Containing Participating Media," Ph.D. Thesis, Univ. of Texas, Austin, TX, 1983.

[5]Naraghi, M. H. N., and Litkouhi, B., "Discrete Exchange Factor Solution of Radiative Heat Transfer in Three-dimensional Enclosures," *Heat Transfer Phenomena in Radiation, Conduction, and Fire*, edited by R. K. Shah, American Society of Mechanical Engineers Publication HTD-Vol. 106, Presented at the National Heat Transfer Conference, Philadelphia, PA, Aug. 6–9, 1989, pp. 221–229.

[6]Fiveland, W. A., "Three-Dimensional Radiative Heat Transfer Solution by the Discrete-Ordinate Method," *Journal of Thermophysics and Heat Transfer*. Vol. 2, No. 4, 1988, pp. 309–316.

[7]Naraghi, M. H. N., and Huan, J., "An N-Bounce Method for Analysis of Radiative Transfer in Enclosures with Anisotropically Scattering Media," *Journal of Heat Transfer*, Vol. 113, No. 3, 1990, pp. 774–777.

[8]Mengüç, M., and Viskanta, R., "Radiative Transfer in Three-Dimensional Rectangular Enclosures, *Journal of Quantitative Spectroscopy and Radiative Heat Transfer*, Vol. 33, 1985, pp. 533–549.

[9]Saltiel, C., and Naraghi, M. H. N., "Analysis of Radiative Heat Transfer in Participating Media Using Arbitrary Nodal Distribution," *Numerical Heat Transfer*, Vol. 17, 1990, pp. 227–243.

[10]Saltiel, C., and Naraghi, M. H. N., "Combined-Mode Heat Transfer in Radiatively Participating Media Using the Discrete Exchange Factor Method with Finite Elements," Heat Transfer 1990, Hemisphere Publishing Corp., Vol. 6, pp. 391–396.

Transient Heat-Pipe Modeling: A Quasisteady, Incompressible Vapor Model

W. Jerry Bowman*
Air Force Institute of Technology, Wright-Patterson Air Force Base, Ohio 45433
and
Robert C. Winn† and Harold L. Martin‡
U. S. Air Force Academy, Colorado Springs, Colorado 80840

Introduction

MANY approaches have been taken regarding the numerical modeling of transient heat-pipe vapor phenomena. The most complicated models assume the vapor flow is two-dimensional, compressible, and unsteady.[1-4] These models are useful in understanding the detailed physics of vapor transients; unfortunately, they require the use of large amounts of computer time. Simpler approaches that model the flow as one-dimensional but still compressible and unsteady have been shown to save great amounts of computer time while still adequately modeling the heat-pipe vapor behavior.[5-8] Methods of accelerating the solution process by using local time-stepping techniques have proved effective in saving computer time when the one-dimensional models are used.[9] All of the models mentioned above have assumed the vapor behaves like an ideal gas. This assumption has often been questioned, but an alternative approach has never been presented.

For the vapor model described in this paper, the vapor flow is assumed to be one-dimensional, compressible in time, incompressible in space, and quasisteady. The vapor is not assumed to be an ideal gas, but is assumed to be a saturated vapor. By assuming the flow is incompressible in the spatial coordinate, and the vapor is a saturated vapor, the vapor modeling problem is greatly simplified. This means both the vapor density and temperature are spatially constant and dependent. As shown below, the transient is modeled by keeping track of the mass and energy leaving and entering the vapor space. At any time during the transient, the vapor velocity distribution and pressure distribution along the heat-pipe can be found, but unlike earlier models, they aren't required as part of the solution process. This saves a great deal of computer time.

Numerical Model

The Wall Model

The transient energy conduction in the heat-pipe wall is modeled by solving the two-dimensional, constant properties, transient, heat diffusion equation. For this work, an explicit, finite difference solution technique is used[10]; however, other methods should work equally well. The temperature of the heat-pipe's external evaporator surface is specified as a boundary condition. A zero temperature gradient is specified as the boundary condition along the external surface of the adiabatic section. A convection boundary condition is used on the external condenser surface. The condenser external environment temperature is specified as part of that boundary condition.

Received March 20, 1991; revision received Sept. 1, 1991; accepted for publication Oct. 5, 1991.

*Associate Professor of Aeronautics. Member AIAA.
†Professor of Aeronautics. Associate Fellow AIAA.
‡Assistant Professor of Aeronautics.